Precipitation Behavior of B_2O_3 Addition on $CaO–Al_2O_3–Sc_2O_3$ Slag System Through in Situ Observation

Fei Wang, Wenke Zhi, Ling Zhang, Zhuangzhuang Liu, Yongnian Dai, Bin Yang and Muxing Guo

Abstract This study focuses on the recycling of scandium from high-temperature processing metallurgical slags through pyrometallurgical routes. For the optimization of the rare earth (scandium) recycling route, the distribution of scandium in $CaO–Al_2O_3–Sc_2O_3$ slag system is worth investigation, and the precipitation behavior of scandium in $CaO–Al_2O_3–Sc_2O_3$ slag system during slag cooling progress is of significance. In this work, the precipitation and solidification behaviors were recorded by a confocal scanning laser microscope (CSLM) combined with an infrared imaging furnace heating (IIF). The compositions and microstructures of the equilibrated phases of these systems were determined by an electron probe microanalyzer with standardized wavelength dispersive spectroscopy (EPMA/WDS). It is observed that there is a remarkable influence of B_2O_3 addition on the precipitation and solidification behaviors in the $CaO–Al_2O_3–Sc_2O_3$ system. By choosing different cooling rates (20, 50, and 100 K/min) the CCT diagram was constructed, which can be employed to guide the rare earth recovery in industrial practice.

Keywords In situ observation · Precipitation · Solidification · $CaO–Al_2O_3–Sc_2O_3$

F. Wang · W. Zhi · Y. Dai · B. Yang
State Key Laboratory of Complex Nonferrous Metal Resources Clear Utilization, National Engineering Laboratory for Vacuum Metallurgy, Key Laboratory for Nonferrous Vacuum Metallurgy of Yunnan Province, Kunming University of Science and Technology, Kunming 650093, Yunnan, People's Republic of China

L. Zhang · Z. Liu · M. Guo
Department of Materials Engineering, KU Leuven, Kasteelpark Arenberg 44 Bus 2450, 3001 Leuven, Belgium
e-mail: muxing.guo@kuleuven.be

B. Yang (✉)
National Engineering Laboratory for Vacuum Metallurgy, Kunming University of Science and Technology, Kunming 650093, Yunnan, People's Republic of China
e-mail: kgyb2005@126.com

Z. Peng et al. (eds.), *11th International Symposium on High-Temperature Metallurgical Processing*, The Minerals, Metals & Materials Series,
https://doi.org/10.1007/978-3-030-36540-0_46

Introduction

Rare earth sesquioxides (RE_2O_3, RE = rare earth) are important compounds in various applications, such as microelectronic, optoelectronic, and optical devices [1–8]. Rare earths are recognized as critical raw materials due to their increasing demands and supply shortages, and the recycling of rare earth elements from end-of-life REEs-containing products are put forward [9, 10]. At present, there are two main methods for recovering rare earth, which are pyrometallurgical and hydrometallurgical [11]. As a traditional method, hydrometallurgy will use a large amount of acid which will produce a large amount of waste acid, wastewater that are serious pollution to the environment. Morais et al. [12] studied the recovery of europium and yttrium from colour TV screens using sulphuric acid as the leaching agent. In this study, the Eu and Y solubilisation was 90 and 95 wt%, respectively, when conducted at 363 K, 2 h of leaching, acid/sample ratio of 1000 kg/t and 40% solids. At 343 K, 1500 kg/t acid/sample ratio, 2 h of leaching, and 40% solids, the solubilisation of both metals was 80%. On the contrary, the combination with pyrometallurgy is considered to be an alternative route; it has a potentially lower impact on the environment and economy [11]. It has the following advantages: short time, less water consumption, high capacity and no restrictions on the recovered rare earth. Muller and Friedrich [13] used $CaO–SiO_2–CaF_2$ slag system to absorb nearly 100 pct of the REs, resulting in 50 to 60 pct RE-containing slag.

B_2O_3,which is commonly used as fluxing agent in metallurgy [14] has remarkable influence on the melting and precipitation behavior in high-processing metallurgical slag. The present research focuses on the recycling of rare earths through pyrometallurgical routes. In order to optimize the recycling route, the distribution of rare earth elements in slag and the precipitation behavior of rare earth elements during slag solidification are important.

From previous studies [15], we know that the phase relations of the $CaO–Al_2O_3–Sc_2O_3$ system and two possible REE recycling schemes. In this paper, it aims to investigate precipitation and solidification behavior of the $CaO–Al_2O_3–Sc_2O_3$ ternary system through in situ CSLM observation. In addition, the CSLM experiment was also carried out on the ternary system with an addition of B_2O_3, so that it optimizes the cooling process for high-REEs recovery. Study of the precipitation behavior of the slag can help in understanding the enrichment and precipitation of rare earth in the slag.

Experimental

Sc_2O_3 (99.999 wt%), CaO (99.9 wt%), Al_2O_3 (99.9 wt%), and B_2O_3 (99.9 wt%) are used as the raw materials, as shown in Table 1. For the quaternary $CaO–Al_2O_3–Sc_2O_3$-B_2O_3 system, 20 wt% B_2O_3 and 30 wt% B_2O_3 were added to the ternary

Table 1 Initial component partition ratio of samples

Sample	CaO (wt%)	Al_2O_3 (wt%)	Sc_2O_3 (wt%)	B_2O_3 (wt%)
1	20	30	50	20
2	20	30	50	30

sample, respectively. The selected slags were prepared according to the isothermal-quenching procedure at 1773 K. The slag samples were placed in the platinum (Pt)-20% rhodium (Rh) crucible on the sample holder inside the confocal scanning laser microscope (CSLM) heating chamber. The temperature calibration was performed using pure copper, nickel and palladium, separately, as references and the sample's temperature was observed to be 358 ± 5 K lower than the measured temperature using the thermocouple. Before the experiment began, CSLM chamber was evacuated and flushed with argon three times. During the experiment, a constant rate of argon (AR) was continuously injected into the gas. The two slag samples have four CSLM experiments of heating and cooling, and their heating and cooling rates are increased from 20, 50, and 100 K/min, respectively. The laser-scanned images of this heating and cooling process were captured and used for further investigation.

For microstructure and phase composition analysis, the samples after the CSLM experiments were embedded in epoxy resin and polished. In order to analyze the microstructure and phase composition better, these samples were coated with either a gold or graphite thin layer to obtain a good surface conductivity. The samples were then analyzed by an electron probe microanalyzer (EPMA, JEOL JXA-8530F) equipped with standardized wavelength dispersive spectroscopy (WDS) and operated at 15 kV and a probe current of 10 nA was performed. The standard samples are CaO, Al_2O_3, Sc_2O_3, and B_2O_3. The average accuracy of EPMA measurements on the main elements is ± 1 wt%.

Results and Discussion

According to the previous studies [15], there are two possible schemes to recover REEs: precipitation of high REEs solid phase in $Ca_2Sc_6Al_6O_{20}$–L region and concentrating of REEs in CaO·Sc_2O_3–L region, respectively. By collecting any of these precipitates from the slag, a REE-rich product can be obtained, which can be used as a rich REE input stream for the next step in the REE recovery process. In order to further prove its feasibility and to study the effect of B_2O_3 on the slag sample, 20 wt% B_2O_3 and 30 wt% B_2O_3 were selected to be added to the sample. The CSLM experiments were carried out on these slag samples. There are lower rare earth elements in metallurgical slags, which can be enriched by changing different cooling trajectory. Therefore, the slag samples quenched at 1773 K were selected for CSLM experiment. At 1773 K, the sample was remelted in the heating chamber, and then cooled at different cooling rates of 20, 50, and 100 K/min, respectively. The slag was

transparent before the first phase precipitates, the collection of the precipitates was detected by holding the focus of the microscope at the bottom of the crucible, by the appearance and the new structure in the liquid.

Through CSLM experiment, the change of cooling process during the experiments was obtained, as shown in the Figs. 1, 2, 3, 4, 5, and 6, respectively. Only the main images of this process were given (some representative images were selected),the composition and microstructure of the precipitates are further confirmed by EPMA/WDS with the back scattering electron (BSE) images of the equilibrated samples, as shown in Fig. 7a. The presence of $Ca_2Sc_6Al_6O_{20}$ and Sc_2O_3 were determined at 1773 K by quantification analysis through EPMA/WDS. In Figs. 1, 3, and 5, with the increase of cooling rate, the slag samples can be completely precipitated in a very short time. It can be explained that under certain conditions of B_2O_3, increasing cooling rate can reduce the time and temperature of complete precipitation. In Figs. 2, 4, and 6, with the increase of cooling rate, the time of complete precipitation of slag samples is shorter than that of Figs. 1, 3, and 5. It can be explained that the cooling rate and the addition of B_2O_3 have a great influence on the complete precipitation of the slag samples. The new precipitate samples prefer to form at the grain boundaries of the crucible. The BSE image of the samples indicates that the precipitate has a

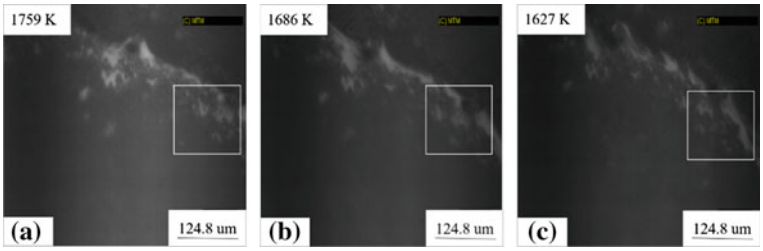

Fig. 1 Slag system samples of 30 wt% Al_2O_3-50 wt% Sc_2O_3-20 wt% CaO-20 wt% B_2O_3, cooling rate at 20 K/min: **a** first precipitates appearing; **b** second type of precipitate appearing; **c** complete solidification

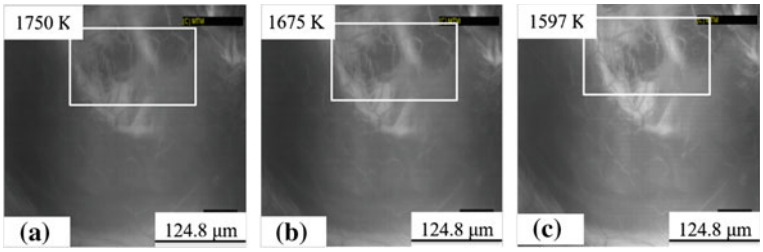

Fig. 2 Slag system samples of 30 wt% Al_2O_3-50 wt% Sc_2O_3-20 wt% CaO-20 wt% B_2O_3, cooling rate at 20 K/min: **a** first precipitates appearing; **b** second type of precipitate appearing; **c** complete solidification

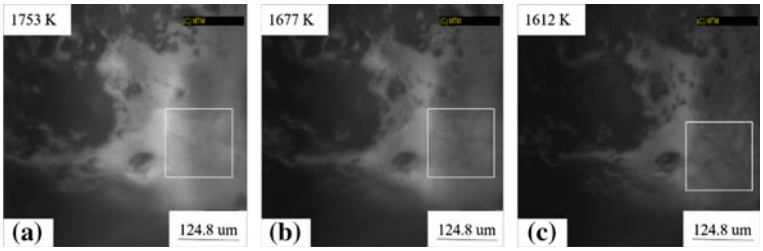

Fig. 3 Slag system samples of 30 wt% Al_2O_3-50 wt% Sc_2O_3-20 wt% CaO-20 wt% B_2O_3, cooling rate at 50 K/min: **a** first precipitates appearing; **b** second type of precipitate appearing; **c** complete solidification

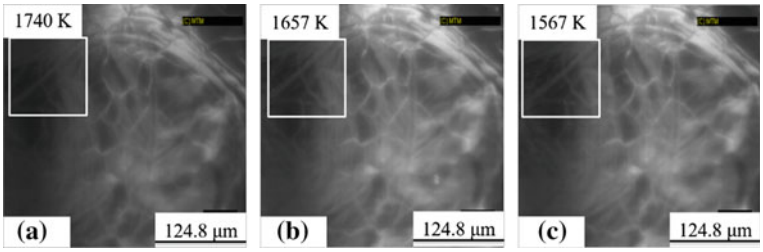

Fig. 4 Slag system samples of 30 wt% Al_2O_3-50 wt% Sc_2O_3-20 wt% CaO-30 wt% B_2O_3, cooling rate at 50 K/min: **a** first precipitates appearing; **b** second type of precipitate appearing; **c** complete solidification

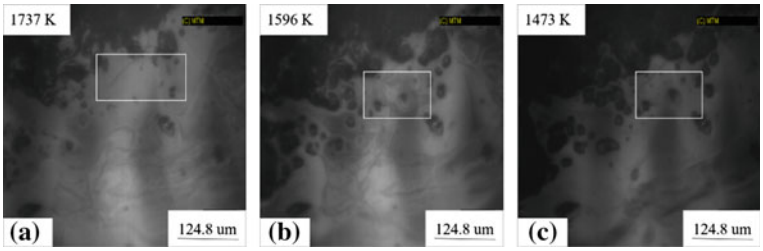

Fig. 5 Slag system samples of 30 wt% Al_2O_3-50 wt% Sc_2O_3-20 wt% CaO-20 wt% B_2O_3, cooling rate at 100 K/min: **a** first precipitates appearing; **b** second type of precipitate appearing; **c** complete solidification

uniform phenomenon (Fig. 7b). In particular, in Figs. 2, 4, and 6a, b, the new precipitate samples prefer to form at the grain boundaries of the crucible. The BSE image of the samples indicates that the precipitate has a uniform phenomenon (Fig. 7c). In addition, no other type of precipitate was further formed during the cooling of the slag, which is in good agreement with the compositional analysis (Fig. 7).

Comparisons between Figs. 1 and 2, when the cooling rate is 20 K/min, the slag sample (30 wt% Al_2O_3-50 wt% Sc_2O_3-20 wt% CaO-30 wt% B_2O_3) has a shorter

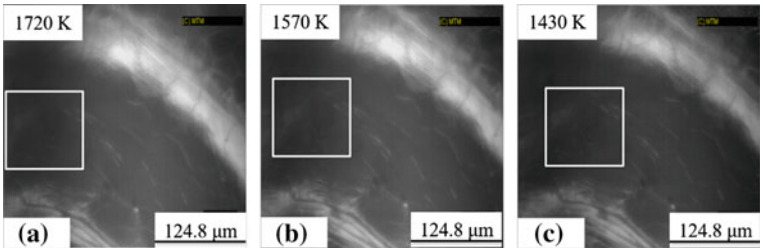

Fig. 6 Slag system samples of 30 wt% Al_2O_3-50 wt% Sc_2O_3-20 wt% CaO-30 wt% B_2O_3, cooling rate at 100 K/min: **a** first precipitates appearing; **b** second type of precipitate appearing; **c** complete solidification

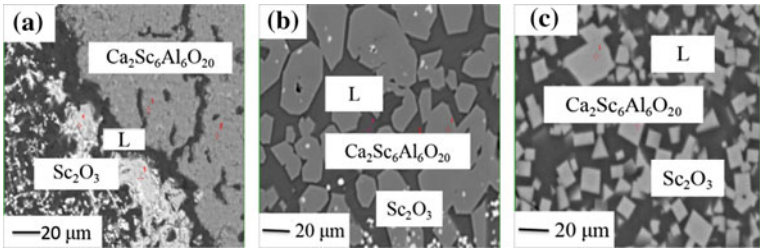

Fig. 7 BSE images of the quenched slag samples from equilibrium at 1773 K. **a** Slag system samples of 30 wt% Al_2O_3-50 wt% Sc_2O_3-20 wt% CaO; **b** Slag system samples of 30 wt% Al_2O_3-50 wt% Sc_2O_3-20 wt% CaO-20 wt% B_2O_3; **c** Slag system samples of 30 wt% Al_2O_3-50 wt% Sc_2O_3-20 wt% CaO-30 wt% B_2O_3

precipitation time and a lower temperature, which indicates that B_2O_3 plays a good role as flux. Comparisons between Figs. 3 and 4, when the cooling rate is 50 K/min, the slag sample (30 wt% Al_2O_3-50 wt% Sc_2O_3-20 wt% CaO-30 wt% B_2O_3) has a shorter precipitation time and a lower temperature than the slag sample (30 wt% Al_2O_3-50 wt% Sc_2O_3-20 wt% CaO-20 wt% B_2O_3), which indicates that B_2O_3 promotes sample precipitation and temperature reduction. Comparisons between Figs. 5 and 6, when the cooling rate is 100 K/min, the slag sample (30 wt% Al_2O_3-50 wt% Sc_2O_3-20 wt% CaO-30 wt% B_2O_3) has a shorter precipitation time and a lower temperature than the slag sample (30 wt% Al_2O_3-50 wt% Sc_2O_3-20 wt% CaO-20 wt% B_2O_3), which indicates that B_2O_3 plays a good role as flux. In addition, in Figs. 1, 2, 3, 4, 5, and 6a, the first image represents the sample in a first precipitates appearing at the indicated temperature, square frames were used to mark visible precipitates, which appear as a brighter or darker color, depending on their positions. In Figs. 1, 2, 3, 4, 5, and 6b, the image shows a second type of precipitate appearing in the ternary slag. As the temperature decreased, this image represents a complete precipitation of the sample, as shown in Figs. 1, 2, 3, 4, 5, and 6c.

With the increase of cooling rate, the slag samples reach complete precipitation at a certain time. Suitable slag composition, cooling rate, and process optimization can be selected for rare earth recovery companies. CSLM experiments and EPMA analysis

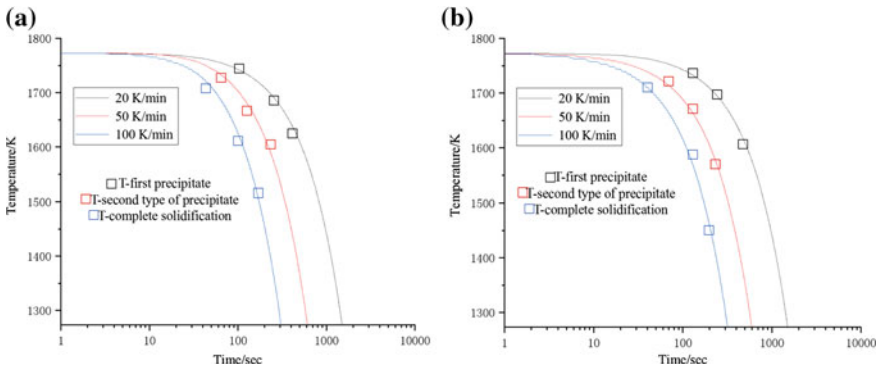

Fig. 8 **a** Precipitation and complete solidification temperatures of 30 wt% Al_2O_3-50 wt% Sc_2O_3-20 wt% CaO-20 wt% B_2O_3 slags and **b** 30 wt% Al_2O_3-50 wt% Sc_2O_3-20 wt% CaO-30 wt% B_2O_3 slags with cooling rate at a: a: 20 K/min b: 50 K/min c: 100 K/min

will be done at different cooling rates and different compositions. In Figs. 1, 2, 3, 4, 5, and 6, first precipitates appearing, second type of precipitate appearing and complete precipitation are seen, which provides a potential reference for the construction of continuous cooling transition (CCT) diagram, as shown in Fig. 8a, b, the results show that the addition of B_2O_3 has a significant effect on the precipitation behavior of slag composition, and also reduces the liquidus and solid-phase temperature of slag; it was a practical tool for the REE recyclers to select appropriate slag compositions and cooling rates and to optimize the process.

Conclusion

Under the conditions of 30 wt% Al_2O_3-50 wt% Sc_2O_3-20 wt% CaO-20 wt% B_2O_3 and 30 wt% Al_2O_3-50 wt% Sc_2O_3-20 wt% CaO-30 wt% B_2O_3 with cooling rates of 20, 50, and 100 K/min, respectively, the precipitation of rare earth-rich compounds was observed in situ. When B_2O_3 is a certain amount, increasing the cooling rate can promote the precipitation and temperature reduction of the slag samples. When the cooling rate is constant, increasing the amount of B_2O_3 can promote the precipitation and temperature reduction of slag samples. It can be seen from this that the process of recovering rare earth from waste containing rare earth can be found by choosing appropriate additives. In addition, the solidification and precipitation behavior resulting from the change of cooling path shows that the efficiency of rare earth recovery and slag recycling can be improved by the reasonable design of slag treatment process.

Acknowledgements Academician Free Exploration Fund of Yunnan Province, China (No.2019HA006) and NSFC-FWO exchange project (Grant No. 5171101430).

References

1. Hong M, Kwo J, Kortan AR, Mannaerts JP, Sergent AM (1999) Epitaxial cubic gadolinium oxide as a dielectric for gallium arsenide passivation. Science 283:1897–1900
2. Kwo J, Hong M, Kortan AR, Queeney KT, Chabal YJ, Mannaerts JP, Boone T, Krajewski JJ, Sergent AM, Rosamilia JM (2000) High ε gate dielectrics Gd_2O_3 and Y_2O_3 for silicon. Appl Phys Lett 77:130–132
3. Becker R, Hartwig H, Köppe H, Vanecek H, Velic P, Warncke R, Gmelin Zelle A (1978) Handbuch der Anorganischen Chemie. Springer, Berlin
4. Petermann K, Fornasiero L, Mix E, Peters V (2002) High melting sesquioxides: crystal growth, spectroscopy, and laser experiments. Opt Mater 19:67–71
5. Heitmann W (1973) Reactively evaporated films of scandia and yttria. Appl Opt 12:394–397
6. Laversenne L, Guyot Y, Goutaudier C, Cohen-Adad MT, Boulon G (2001) Optimization of spectroscopic properties of Yb^{3+}-doped refractory sesquioxides: cubic Y_2O_3, Lu_2O_3 and monoclinic Gd_2O_3. Opt Mater 16:475–483
7. Zarembowitch J, Gouteron J, Lejus AM (1980) Raman spectrum of single crystals of monoclinic B-type gadolinium sesquioxide[J]. J Ramin Spectrosc 9:263–265
8. Jüstel T, Krupa JC, Wiechert DU (2001) VUV spectroscopy of luminescent materials for plasma display panels and Xe discharge lamps. J Lumin 93:179–189
9. Binnemans K, Jones PT, Blanpain B, Gerven TV, Yang Y, Walton A, Buchert M (2013) Recycling of rare earths: a critical review. J Clean Prod 51:1–22
10. Massari S, Ruberti M (2013) Rare earth elements as critical raw materials: Focus on international markets and future strategies. Res Policy 38:36–43
11. Le TH, Malfliet A, Blanpain B, Guo M (2016) Phase relations of the $CaO–SiO_2–Nd_2O_3$ system and the implication for rare earths recycling. Metall Mater Trans B 47:1736–1744
12. De Morais C (2000) Recovery of europium and yttrium from color TV tubes//55 Congresso Anual Associacao Brasileria de Metalurgia e Materiais, Rio de Janeiro, Brazil, p 24
13. Müller T, Friedrich B (2006) Development of a recycling process for nickel-metal hydride batteries. J Power Sour 158:1498–1509
14. Wang HM, Yang LL, Zhu H, Yan YQ (2011) Comparison of effects of B_2O_3 and CaF_2 on metallurgical properties of high basicity CaO-based flux//Advanced Materials Research. Trans Tech Publ 311:966–969
15. Zhi W, Wang F, Yang B, Qu T, Deng Y, Tian Y, Zhao J (2019) Phase relations of $CaO–Al_2O_3–Sc_2O_3$ ternary system. J Am Ceram Soc 102:2863–2870